Modeling Study of Peripheral Nerve Recording Selectivity

Javier Perez-Orive and Dominique M. Durand, *Member, IEEE*

***Abstract*—Recording of sensory information from afferent fibers can be used as feedback for the closed-loop control of neural prostheses. Clinical applications suggest that recording selectively from various nerve fascicles is important. Current nerve cuff electrodes are generally circular in shape and use a tripolar recording configuration. Preliminary experiments suggest that slowly changing the shape of the nerve to a flatter cross section can improve its selectivity. The objective of this work is to determine the effects of nerve reshaping and other cuff design parameters on the fascicular recording selectivity of a nerve cuff. A finite-element computer model of a multifasciculated nerve with different cuff electrodes was implemented to simulate the recordings. The model included the inhomogeneous and anisotropic properties of peripheral nerves. The recording selectivity was quantified with the use of a Selectivity Index. The results from the model provided information regarding the effect of using monopolar versus tripolar recording configurations, the length of the tripoles in tripolar recordings, the number of contacts that maximize the selectivity index, and the cuff length. Nerve reshaping was found to cause important recording selectivity improvements (106% average). These results provide specific criteria for the design of selectively recording nerve cuff electrodes.**

I. Introduction

NEURAL prostheses seek to restore function to neurologically impaired individuals by using functional electrical stimulation (FES) in order to electrically activate the nervous system [1], [28]. Closed-loop control with appropriate sensors can improve the performance of these neural prostheses [3], [7]. However, the use of artificial sensors to provide feedback signals for this control poses several problems such as: donning and doffing times, frequent calibrations, cosmesis, mechanical reliability and biocompatibility [16], [24]. Peripheral nerve recordings of the sensory signals contained in afferent fibers can provide information about variables such as pressure, joint angle, muscle force, or length [11]–[13], [16], [31]. To reduce problems associated with implanting large numbers of recording electrodes, it is necessary for a single electrode to be able to provide selective recordings.

Fascicular recording selectivity is defined as the ability of a nerve electrode to distinguish between different active fascicles based on their spatial location within the nerve. Even though the fascicles in a nerve are known to migrate and intermingle with each other along the length of the nerve, the anatomical evidence indicates that there still is a considerable degree of fiber localization [4], [32], [33]. The localization of fibers coming from a specific branch is usually largest close to the point where the nerve trunk branches [32]. Spatial recording selectivity is based on the fact that signals generated by a localized group of fibers in a nerve will decrease in amplitude as the distance between the recording electrode and the fibers increases. Spatial selectivity can therefore be used to distinguish between active fascicles.

Several attempts have been made to achieve fascicular recording selectivity with cylindrical nerve cuff electrodes [8], [14], [22], [30], [19] and achieved good selectivity. However, nerves are not normally round and preliminary experiments suggest that changing the shape of the nerve to a flatter cross section can improve its stimulation selectivity [35]. This flatter cross section could also improve the recording selectivity by allowing larger differences in the voltage distribution within the cuff. Therefore, the goal of this paper is to determine the effect of nerve reshaping on fascicular recording selectivity. The effect of various parameters such as electrode configuration, length of the electrode and number of recording positions on recording selectivity was quantified with the use of a selectivity index (SI) originally defined by Chen *et al.* [6] and modified for this analysis. A modeling approach based on finite-element analysis was used in order to take into account the inhomogeneities and anisotropies in the volume conductor.

II. Methods

1) Selectivity Index (SI): Let vector V_i be defined as $V_i = (v_{i1}, v_{i2}, \ldots, v_{iN})$ formed with N elements, v_{ij}, taken from the peak-to-peak amplitudes (p-pAs) of the recording obtained from contact j (out of N possible contacts) while fascicle i is active (out of M possible fascicles), such that M vectors in N-dimensional space are generated. The voltage v_{ij} is first normalized to the average value of all the contacts to eliminate the effect of contact impedance

$$c_{ij} = \frac{v_{ij}}{\sum_{k=1}^{M} v_{kj}}.$$

All vectors are then normalized to unit magnitude for all fascicles: $W_i = (w_{i1}, w_{i2}, \ldots, w_{iN})$ where

$$w_{ij} = \frac{c_{ij}}{\sqrt{c_{i1}^2 + c_{i2}^2 + \cdots + c_{iN}^2}}.$$

Manuscript received June 22, 1999; revised November 15, 1999, January 21, 2000, and May 4, 2000. This work was supported by the NIH-NINDS Grant NS32484 and by a fellowship from the Centro Nacional de Rehabilitacion, Mexico.

The authors are with the Neural Engineering Center, Department of Biomedical Engineering, Case Western Reserve University, Cleveland, OH 44106 USA (e-mail: dxd6@po.cwru.edu).

Publisher Item Identifier S 1063-6528(00)07294-3.

1063–6528/00$10.00 © 2000 IEEE

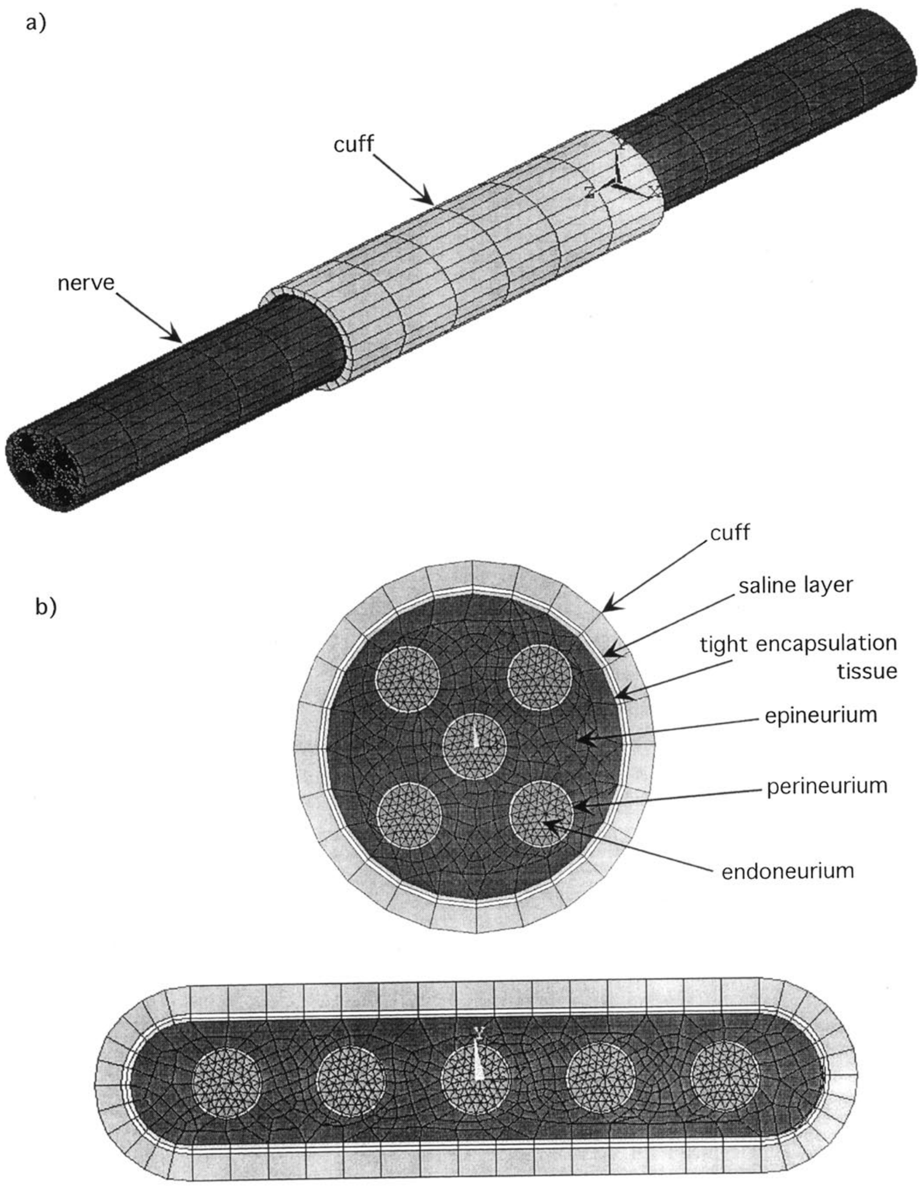

Fig. 1. (a) Three-dimensional finite-element model representation of 1.2-cm-long circular cuff. (b) Cross-sectional areas of finite-element models of circular and flat cuffs surrounding multifasciculated nerves. Both models have the same cross-sectional areas of all nerve tissues and the same thickness of encapsulation tissue layer, saline layer and cuff. The amount of flattening was determined by keeping constant the minimum distance from fascicle to cuff.

With the vectors normalized across contacts and fascicles, the Euclidean distance between the ith and kth vectors is then calculated

$$d_{ik} = \frac{100}{\sqrt{2}} \cdot \sqrt{(w_{i1}-w_{k1})^2+(w_{i2}-w_{k2})^2+\cdots+(w_{iN}-w_{kN})^2}. \quad (1)$$

This distance is normalized as a percentage of the theoretical maximum value obtained when all vectors are orthogonal to each other. The selectivity index for the kth fascicle, S_k, is defined as the average distance between vector W_k and all the other vectors. The selectivity index (SI) of the cuff will be the average of the selectivity indexes for each fascicle

$$\mathrm{SI} = \frac{1}{M}\sum_{k=1}^{M}\left(\frac{1}{M-1}\sum_{i=1,\, i\neq k}^{M} d_{ik}\right). \quad (2)$$

2) Model Implementation: Several models of three-dimensional (3-D) multifasciculated nerves surrounded by cuff electrodes with different lengths and cross-sectional geometries were implemented (Fig. 1). Three different cuff lengths and two cross-sectional geometries were modeled: 1.2-, 2.4-, and 4.8-cm cuff lengths, and circular and flat geometries, respectively. A finite-element modeling software package (Ansys 5.3, Ansys Inc., Canonsburg, PA) was used. The size of the models ranged between 13 396 nodes and 16 976 elements in

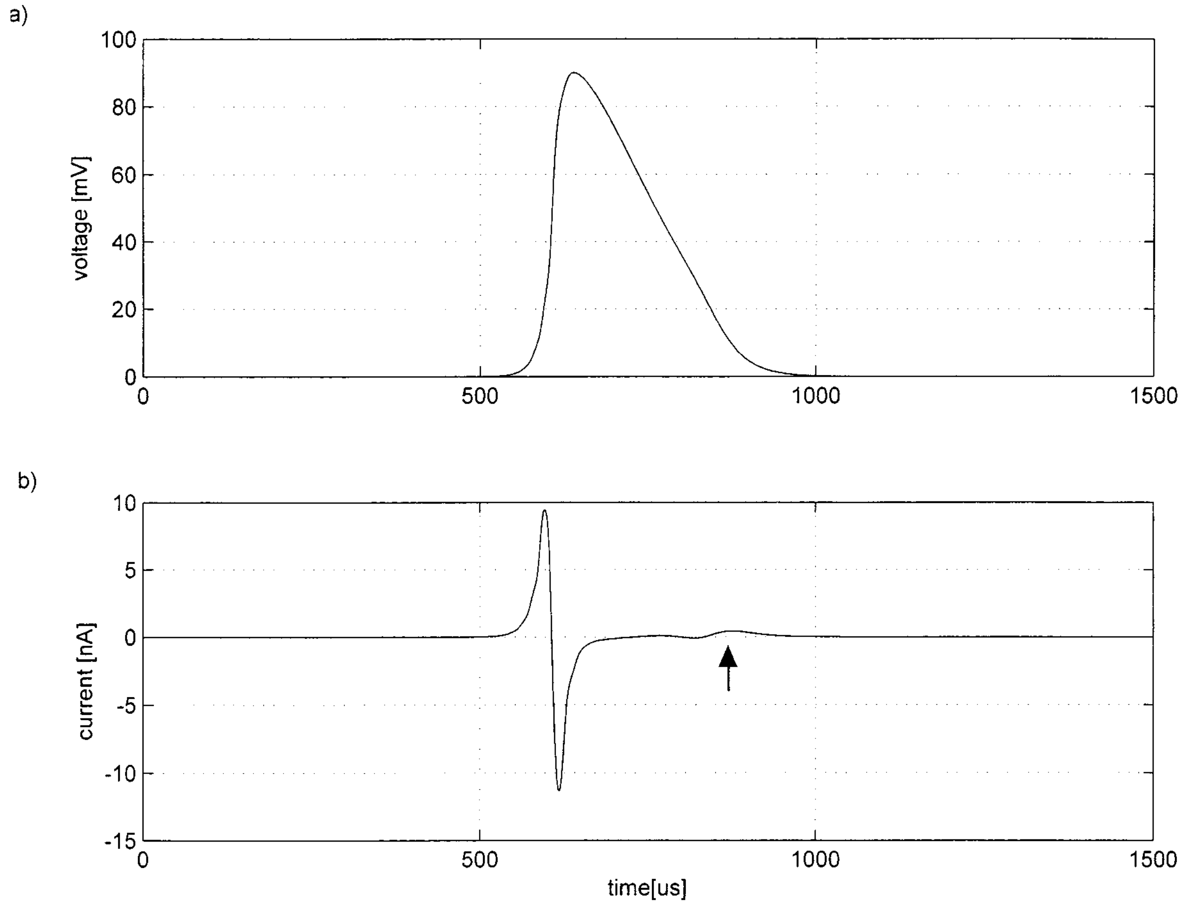

Fig. 2. (a) Waveform of action potential versus time. (b) Waveform of action current (i_m) versus time. These waveforms were obtained with a compartmental cable model using Sweeney kinetics (Hsu and Durand, 1996; Sweeney *et al.*, 1987) of a 20-μm diameter fiber with 2-mm internodal distance. The arrow in (b) indicates the third phase in i_m necessary for the model to produce triphasic recordings. The action current resembles the second derivative of the action potential.

the 1.2 cm cuff model, and 27 580 nodes and 36 074 elements in the 4.8-cm cuff model.

The nerve model consisted of three different tissues with different electrical resistivities: endoneurium (longitudinal $\rho = 1.0$ Ω·m; transverse $\rho = 100$ Ω·m), perineurium ($\rho = 1592$ Ω·m) and epineurium ($\rho = 1.0$ Ω·m). The cuff was modeled with the resistivity of silicone rubber ($\rho = 1 \times 10^{17}$ Ω·m). Between the cuff and the nerve, a layer of tight encapsulation tissue ($\rho = 15.17$ Ω·m) and a layer of saline ($\rho = 0.5$ Ω·m) were placed. The nerve and cuff are immersed in a bath of saline solution. The following model dimensions were used: circular model nerve diameter: 3 mm; fascicle diameter: 617 μm; perineurium thickness: 25 μm; encapsulation tissue thickness: 42 μm; saline layer thickness: 42 μm; silicone rubber cuff thickness: 300 μm; diameter of external saline bath: 40 mm. Longitudinally, the nerve extruded 10 mm from the cuff at both ends. The model dimensions are representative of the sciatic nerve of a cat, an animal model used for nerve recording experiments [16], [24]. To reduce the number of parameters involved and to facilitate the interpretation of the results, the fascicles were positioned equidistant from each other within the cuff, had a similar round shape and diameter. The effect of fascicle diameter on selectivity was studied separately. By varying the cross-sectional geometry of the model, the following variables were kept constant: minimum distance from fascicle to cuff (this feature determined the amount of flattening of the model); cross-sectional areas of endoneurium, perineurium and epineurium; thickness of encapsulation tissue layer, saline layer and cuff. The cross-sectional perimeters increased in the flat cuff model. The voltage was set at 0 V at the boundary of the saline bath surrounding the nerve and cuff. The sizes of the saline bath and of the longitudinal nerve extrusion were chosen to be large enough so that increasing their size further would have a negligible effect on the recordings [5].

Each longitudinal node in the endoneurium section of the finite-element model represents a node of Ranvier in a single fiber. Action potentials were simulated as propagating in a single fiber located in the center of the fascicles. An action potential propagating through an axon was modeled as a series of current sources that represent the current flowing through the cell membrane (i_m) at each node of Ranvier (Fig. 2).

A compartmental cable model with Sweeney active dynamics [17], [33], which include the kinetics of a mammalian myelinated axon, was used to simulate the action potential [Fig. 2(a)] generated by a 20-μm diameter fiber with 2-mm internodal distance. Time steps of 1 μs were used in the model. The membrane current waveform obtained with this model agrees with previous experimental [34] and modeling [9], [20], [28] results. The current sources simulating the i_m waveform were moved along the endoneurium of the finite-element model at discrete

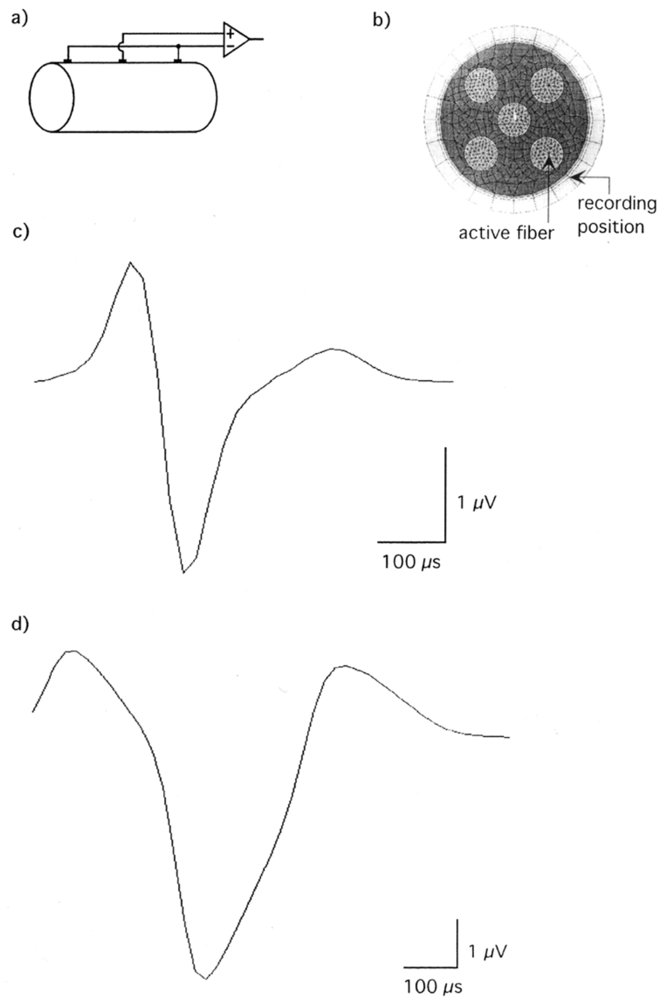

Fig. 3. (a) Diagram of tripolar configuration in cuff model. (b) Arrows indicate locations of active fiber inside fascicle and recording position on interior surface of cuff. (c) Voltage versus time recording with tripolar configuration in 1.2-cm-long circular cuff. (d) Voltage versus time recording with tripolar configuration in 4.8-cm-long circular cuff. The waveforms, amplitudes and durations of the recordings agree with those reported by Stein *et al.*(1975) and Hoffer *et al.* (1981) for single fiber recordings in animal experiments. Recordings from flat cuffs had similar waveforms, durations and amplitudes.

steps that corresponded with the conduction velocity (100 m/s) of the propagating action potential.

Monopolar recordings were simulated by measuring the voltage of a contact with respect to the reference. Tripolar recordings were simulated by subtracting the average of the recordings at the two end contacts from the recording at the central contact [Fig. 3(a)].

III. Results

Two tripolar ENG recordings obtained from 1.2- and 4.8-cm-long circular models are shown in Fig. 3(c) and (d), respectively. The locations of the fiber and of the recording position on the inside surface of the cuff are shown in Fig. 3(b). These waveforms have the same characteristics as single fiber recordings obtained in animal experiments with similar lengths of isolating medium surrounding the nerve [24]: the recorded waveforms are triphasic with the long cuff producing a large third phase and the shorter cuff a small third phase. In the longer cuff, the first and third phase are of similar magnitudes and the second phase is approximately twice as large. The same relationship between the magnitudes of the three phases was obtained experimentally by Stein *et al.* [24]. The p-pA of the waveforms produced by the model ranged between 0.18 μV and 6.59 μV, depending on the recording configuration, the distance between the recording position and the active fascicle, the length and shape of the cuff. The peak-to-peak duration of the waveforms produced by the model ranged between 60 μs and 240 μs, depending on the recording configuration and the length of the cuff. Both the p-pA and the peak-to-peak durations obtained with the model are within the range of values obtained experimentally [14], [24].

1) Effect of Contact Distribution: The effects of tripole length on p-pA and SI are shown in Fig. 4(a). Longer tripoles yield larger p-pA than shorter tripoles [91% average voltage decrease going from longest to shortest tripole for the cuff shown in Fig. 4(a)]. However, longer tripoles produce smaller SI values than shorter tripoles [82% average SI value decrease going from shortest to longest tripole for the cuff shown in Fig. 4(a)]. For a given tripole length, the p-pA are largest for the contact closest to the active fascicle and smallest for the contact farthest from the active fascicle (180°), as expected. Fig. 4(a) also shows that the monopolar recordings behave similarly to the longest tripole. They provide large p-pA, but small SI. Monopolar recordings have no advantage over tripolar recordings: they provide worse selectivity than any tripole length while recording similar p-pA than the long tripoles.

The effect of the number of recording positions on the selectivity index is shown in Fig. 4(b). The figure shows that there is an optimum number of recording positions for maximum selectivity, and that this number depends on the number of fascicles to be distinguished [Fig. 4(b)]. To distinguish between five fascicles, the highest SI is obtained by using four recording positions while distinguishing between two fascicles requires only two recording positions.

2) Effect of Cuff Length: For monopolar recordings, increasing the cuff length increased the p-pA but decreased the SI [Fig. 5(a)]. That is, changing the length of the cuff in a monopolar recording produces similar effects to changing the length of the tripole in a tripolar recording. Conversely, in tripolar recordings varying the length of the cuff while keeping the tripole length constant causes negligible changes (less than 2%) in both p-pA and SI values [Fig. 5(b)].

3) Effect of Nerve Reshaping: Fig. 6(a) shows the average value of the amplitudes at the contacts closest and farthest to the active fascicle for monopolar (M) and tripolar (T) configurations, and 1.2- and 2.4-cm cuff lengths. Changing the cross-sectional geometry of the cuff from circular to flat did not cause significant differences between the average p-pA of the recorded waveforms. However, the amplitude difference from the closest to the farthest contact is always larger for the flat model [see Fig. 6(b) and the error bars of Fig. 6(a)]. This difference suggests that the flat cuff has a less homogeneous voltage distribution than the circular cuff. As a result, the SI values obtained from the flat model were always larger than those for the circular model, regardless of the cuff length, the recording configuration used a)

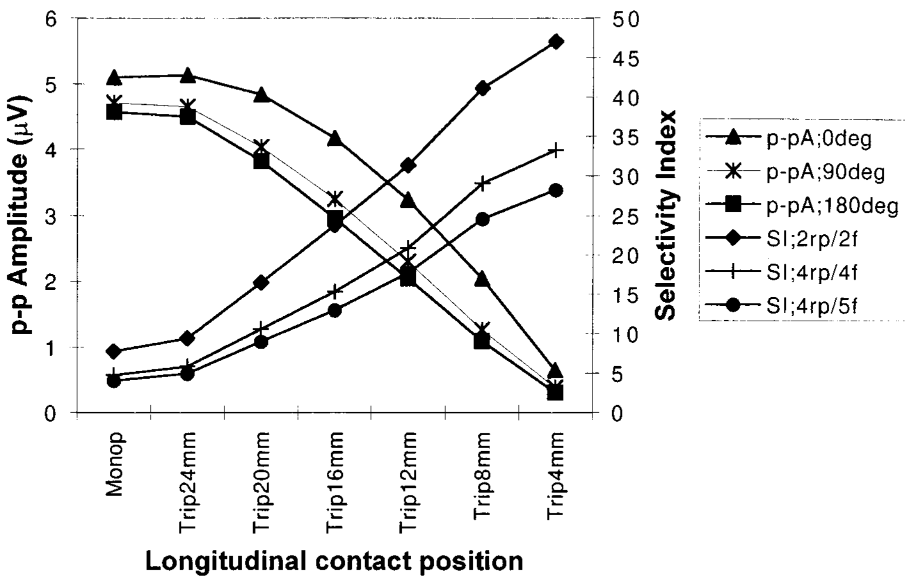

b)

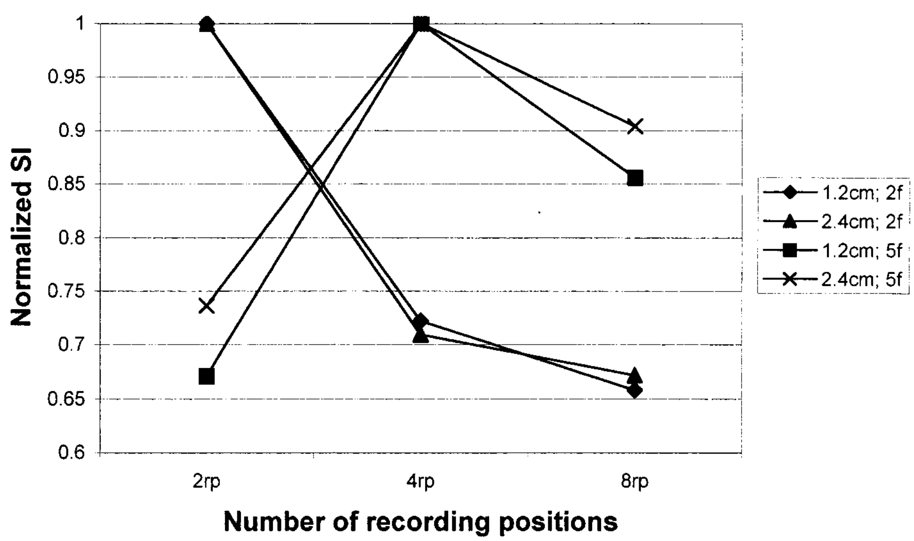

Fig. 4. (a) Effect of tripole length on p-pAand SI for circular model with 2.4-cm cuff length. Values of p-pA are shown for contacts at 0°, 90° and 180° (measured relative to the active fascicle). SI values are shown for two recording positions to distinguish between two fascicles $(2rp/2f)$, and four recording positions to distinguish between four and five fascicles ($4rp/4f$ and $4rp/5f$, respectively). Tripole length has an opposite effect on p-pA and SI. Distinguishing between larger numbers of fascicles decreases the selectivity. All other cuff lengths, as well as the flat nerve geometry, yielded similar results. Values for monopolar recordings are plotted here for easier comparison with tripolar recordings. The monopolar recording configuration produces p-pA values similar to those obtained with the longest tripole available in a given cuff length. SI values for monopolar recordings are smaller than those for any tripole length. (b) Effect of number of recording positions used on the SI for circular cuffs 1.2- and 2.4-cm long. Data are shown for SI while distinguishing between two $(2f)$ and five $(5f)$ fascicles. The optimum number of recording positions to use depends on the number of fascicles to be distinguished.

(monopolar or tripolar) or the number of fascicles distinguished [Fig. 6(c)]. The average SI improvement obtained with the flat cuff in these different recording simulations was 106%. Distinguishing between four or five fascicles did not make a large difference in the selectivity improvements (103% and 109% improvement for four and five fascicles, respectively).

4) Effect of Fiber Diameter and Perineurium Resistivity: To analyze the effect of fiber diameter on the recordings, the action potential generated by a 10-μm diameter fiber was simulated in a finite-element model of a 1.2-cm-long flat cuff. The results from this simulation showed that the amplitudes of the recordings were on average 71% smaller for a 10-μm fiber than for

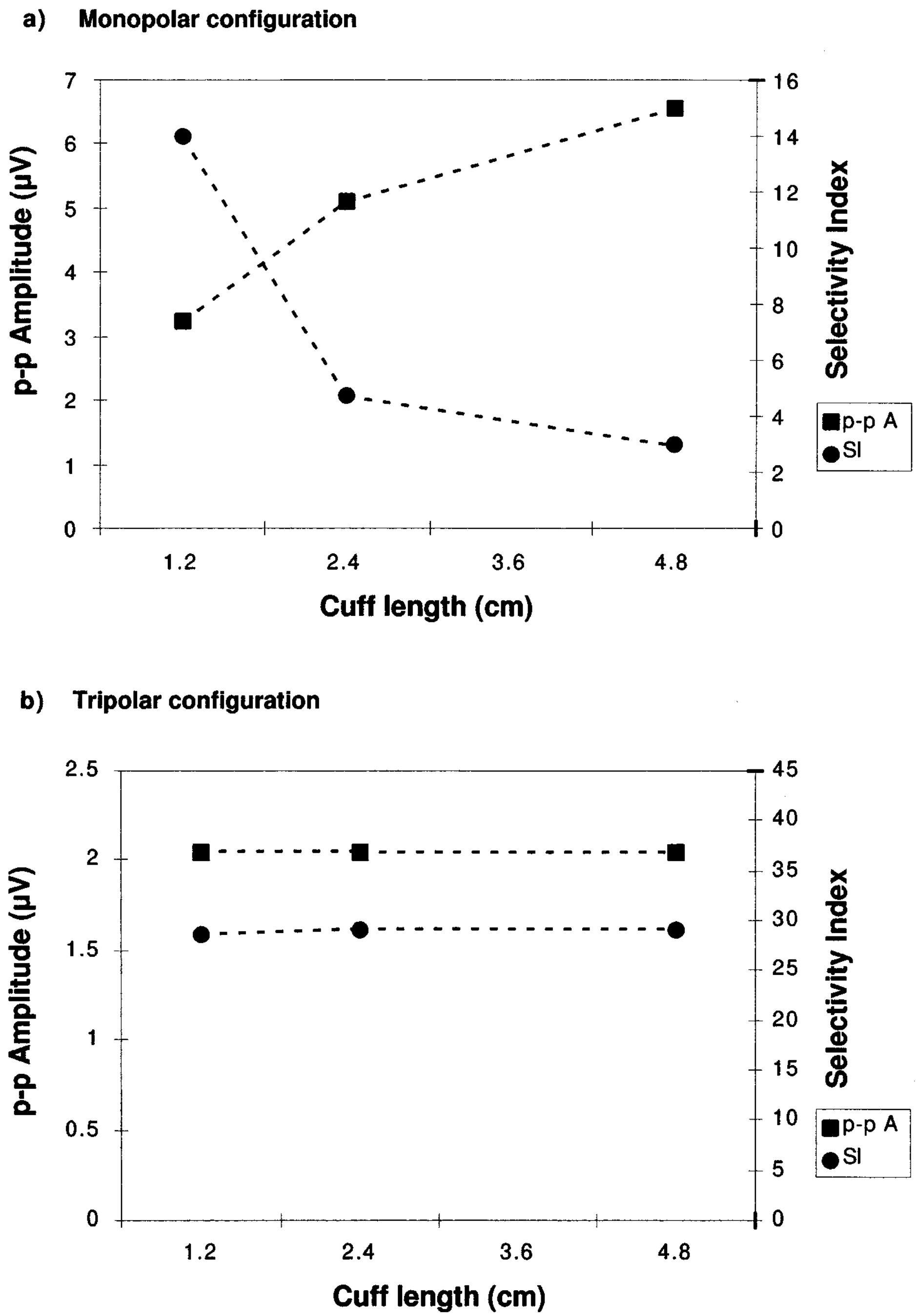

Fig. 5. Effect of cuff length on (a) monopolar and (b) tripolar recordings in circular model. The cuff length has an important effect on monopolar recordings (longer cuffs produce larger p-pA and smaller SI) and a negligible effect on tripolar recordings of a constant tripole length (in the case of this figure, 1.2 cm). Flat cuff model produced similar results.

a 20-μm fiber in a cuff of the same length. However, the results indicate that the cuff design parameters still have the same general effect on the recordings in this model as in the 20 μm diameter fiber models. To investigate the effect of resistivity on the p-pA and SI results, a 2.4-cm-long circular cuff model was implemented where the resistivity of the perineurium was made equal to that of the epineurium (1 Ω·m). Similarly, the results obtained from this model showed that the absence of perineurium caused the average p-pA and SI to increase by 36% and 19%, respectively. However, the cuff design parameters still have the same general effect on these recordings as in the models with normal perineurium resistivity used for all other simulations reported above.

IV. Discussion

A finite-element model of an inhomogeneous anisotropic multifasciculated nerve with different cuff geometries has been implemented. The waveform, amplitude and duration of the recordings obtained from this model agree with single fiber recordings from animal experiments [14], [24]. The simulations performed in this model provide specific criteria for the design of selectively recording nerve cuff electrodes.

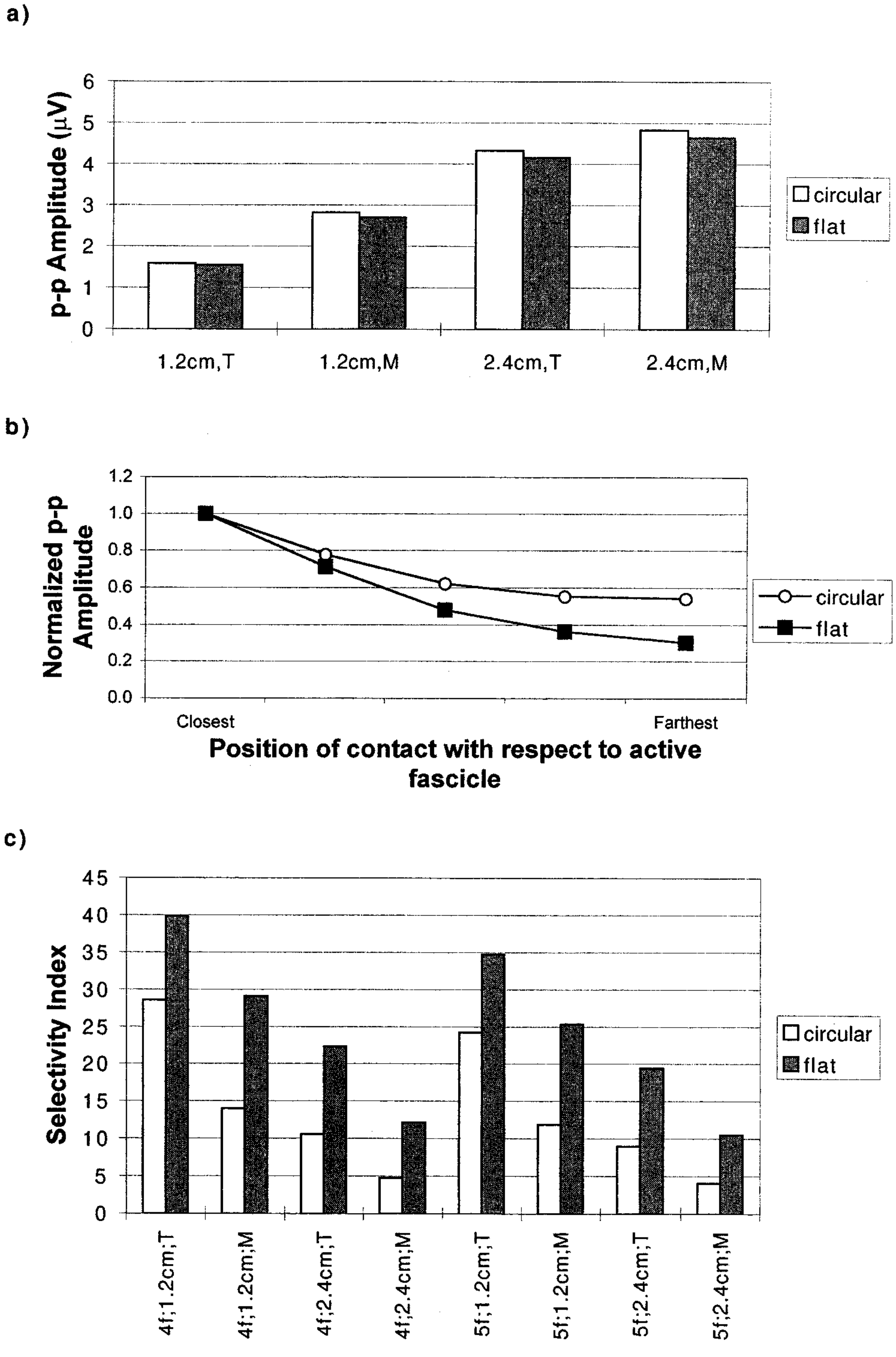

Fig. 6. Effect of nerve reshaping on recordings. (a) The bars represent the average of the amplitudes at the contacts closest and farthest to the active fascicle (these extreme p-pA are shown in the error bars). Amplitudes are shown for 1.2- and 2.4-cm-long cuffs and monopolar (M) and tripolar (T) configurations. Average amplitudes recorded from circular and flat models are similar. (b) Normalized decrease of p-pA from closest to farthest contact for tripolar recordings in 1.2-cm-long circular and flat cuff models. The amplitude differences from closest to farthest contact are larger in the flat model [which can also be seen in the error bars of Fig. 6(a)]. The same relationship was observed for monopolar recordings and other cuff lengths. (c) SI values for circular and flat models while distinguishing between four $(4f)$ or five $(5f)$ fascicles, using 1.2- or 2.4-cm-long cuffs and monopolar (M) or tripolar (T) recording configurations. The SI values for the flat model are always significantly larger than those for the circular model.

Several investigators have modeled the extracellular potential generated by a single fiber in a uniform volume conductor, either infinite [9] or restricted by an isolating medium [2], [19], [26], [28]. These models produced extracellular potential waveforms with characteristics similar to our results. In these models, the effect of the length of the isolating medium was also similar to that reported here [Fig. 3(c) and (d)]. To the best of our knowledge, there has only been one other attempt at modeling the effect of an action potential in an inhomogeneous anisotropic volume conductor resembling the different tissues in a nerve a)

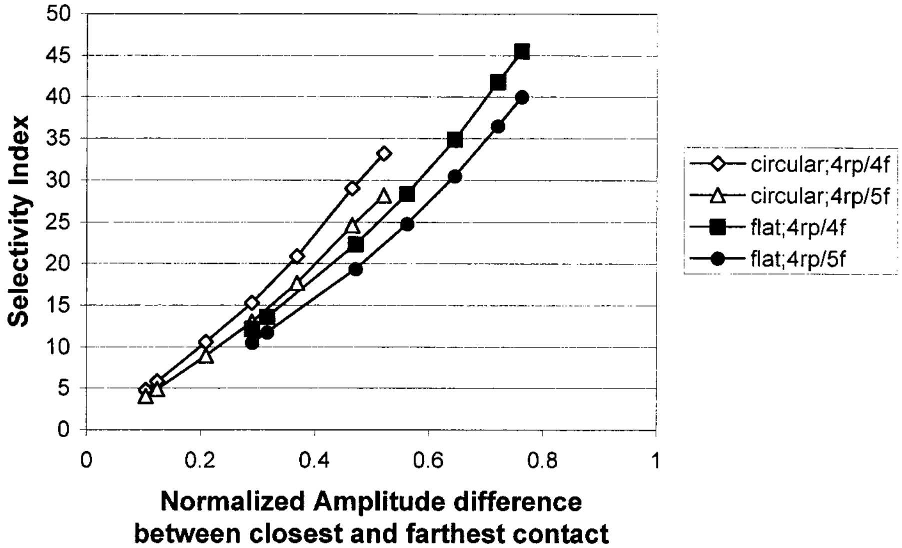

b)

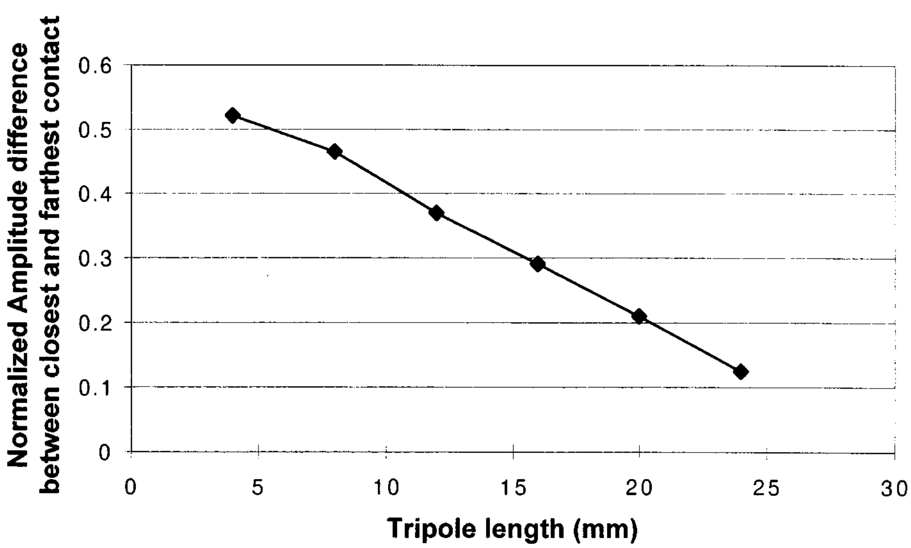

Fig. 7. (a) Relationship between normalized amplitude difference from closest to farthest contact and SI value for circular and flat 2.4-cm-long cuff models. Each series represents a given combination between cuff geometry and number of fascicles to be distinguished. The points in each series are from monopolar and tripolar recordings (of different tripolar lengths). The amplitude difference from closest to farthest contact is strongly related to the SI values. All other cuff lengths showed the same behavior. (b) Relationship between tripole length and normalized amplitude difference from closest to farthest contact for 2.4-cm-long circular cuff model. There is an inverse relationship between tripole length and amplitude difference from closest to farthest contact. The flat cuff model and other cuff lengths showed the same behavior.

trunk: endoneurium, perineurium and epineurium [20]. However, this model focused on studying intrafascicular recordings in a unifascicular nerve. Using finite-element analysis software it is possible to implement models that are not radially symmetric and to include complex inhomogeneities known to be present in peripheral nerves.

An unexpected result is that the number of recording positions for the maximum SI value is related to the number of fascicles that are to be distinguished. This optimum number is not always the highest number of recording positions available. Additional recording positions can provide more information increasing the SI but too much information is redundant and can decrease the SI. In clinical applications, it is unrealistic to expect that the contacts will be always close to specific fascicles. Therefore, implanting cuffs with a larger number of recording positions increases the probability that some of those recording positions will be placed directly above a given fascicle. Once the cuff is implanted and the recording positions that are closest to the fascicles are identified, only a certain number of recording positions should be actually used for the SI to be maximized.

The tripole length results indicate that there is a compromise between signal amplitude and selectivity [Fig. 4(a)]. Similar relationships between tripole length and recorded amplitude have been reported elsewhere [14], [22], [25]. When a recording system provides a satisfactory signal-to-noise ratio (SNR), selectivity can be improved with a shorter tripole length.

The simulation results show that there is a high degree of correlation ($r = 0.996$ for circular cuffs; $r = 0.995$ for flat cuffs) between the amplitude difference from closest to farthest contact and the recording selectivity [Fig. 7(a)]. The normalized amplitude difference from closest to farthest contact was then plotted as a function of tripole length [Fig. 7(b)]. This figure shows a linear relationship with a high inverse correlation ($r = -0.998$), and can explain why short tripole recordings are more selective than long tripole recordings.

It has been suggested [28] that the presence of the cuff decreases selectivity because the cuff's isolating medium makes the electric field within it more homogeneous. Our results indicate that the decrease in selectivity observed in longer cuffs is related to the use of a longer tripole and not to the effects of a longer isolating medium surrounding the nerve. A 4.8-cm-long cuff did not have a more homogeneous electric field within it than a 1.2-cm cuff: the difference between maximum and minimum voltages on the surface of the cuff is 1 μV in both cases (data not shown). Using a short tripole yielded the same high value of SI independent of the length of the cuff where it was used [Fig. 5(b)].

The modeling results also indicate that changing the shape of the nerve by using a cuff with a flatter cross section can double the recording selectivity without decreasing signal amplitude. Chronic experiments with these electrodes implanted on the sciatic nerves of rats for three months have revealed that the reshaping of these nerves can be done with little or no damage [35]. Three types of cuffs applying small, medium or large initial pressure to the nerve were tested. The results show that an electrode that applies only a small amount of pressure can flatten the nerve and the fascicles without any observable histological or physiological damage. Cuffs with higher pressure produced a small amount of demyelination and regeneration. The flat cuff produced similar selectivity improvements while distinguishing between four (103%) or five (109%) fascicles. Hence, the main factor involved in the selectivity improvement is not the fact that the position of the fifth fascicle (which is the central fascicle in the circular cuff model) but rather that the flat cuff produces larger amplitude differences from closest to farthest contact.

Once a cuff has been implanted around a nerve, there still remains the task of predicting which fascicle is active from the recordings obtained at the different recording positions. Christensen *et al.* [8] used discriminant analysis to identify which cat digit had been mechanically stimulated while selectively recording from the median and ulnar nerves. The results using their cuff design show that identification accuracy is 71–92% and a correlation coefficient of 0.79 between SI and percentage accuracy of identification. Based on these findings, our results suggest that a high percentage of accurate identification is feasible with these cuff designs.

REFERENCES

[1] W. F. Agnew and D. B. McCreery, Eds., *Neural Prostheses: Fundamental Studies*. Englewood Cliffs, NJ: Prentice Hall, 1990.

[2] L. N. S. Andreasen, J. J. Struijk, and M. Haugland, "An artificial nerve fiber for evaluation of nerve cuff electrodes," in *Proc. 19th IEEE/EMBS Annu. Int. Conf.*, 1997.

[3] B. J. Andrews, R. H. Baxendale, R. Barnett, G. F. Phillips, T. Yamazaki, J. P. Paul, and P. A. Freeman, "Hybrid FES orthosis incorporating closed loop control and sensory feedback," *J. Biomed. Eng.*, vol. 10, pp. 189–195, 1987.

[4] C. R. Bardeen, "Development and variation of the nerves and the musculature of the inferior extremity and of the neighboring regions in man," *Amer. J. Anat.*, vol. 6, pp. 1906–1907, 1906–1907.

[5] J. K. Cavanaugh, J.-C. Lin, and D. M. Durand, "Finite element analysis of electrical nerve stimulation," in *Proc. 18th IEEE/EMBS Annu. Int. Conf.*, 1996.

[6] Y. Chen, P. R. Christensen, K. D. Strange, and J. A. Hoffer, "Multichannel recordings from peripheral nerves: 2. Measurement of selectivity," in *Proc. IFESS/NP*, 1997, pp. 241–242.

[7] H. J. Chizeck, P. E. Crago, and L. S. Kofman, "Robust closed-loop control of isometric muscle force using pulse width modulation," *IEEE Trans. Biomed. Eng.*, vol. 35, pp. 510–517, 1988.

[8] P. R. Christensen, Y. Chen, K. D. Strange, K. Yoshida, and J. A. Hoffer, "Multi-channel recordings from peripheral nerves: 4. Evaluation of selectivity using mechanical stimulation of individual digits," in *Proc. IFESS/NP*, 1997, pp. 217–218.

[9] J. Clark and R. Plonsey, "The extracellular potential field of the single active nerve fiber in a volume conductor," *Biophys. J.*, vol. 8, pp. 842–864, 1968.

[10] M. Haugland, J. A. Hoffer, and T. Sinkjaer, "Skin contact force information in sensory nerve signals recorded by implanted cuff electrodes," *IEEE Trans. Rehab. Eng.*, vol. 2, pp. 18–28, 1994.

[11] M. Haugland, A. Lickel, J. Haase, and T. Sinkjaer, "Control of FES thumb force using slip information obtained from the cutaneous electroneurogram in quadriplegic man," *IEEE Trans. Rehab. Eng.*, vol. 7, pp. 215–227, 1999.

[12] M. Haugland and T. Sinkjaer, "Cutaneous whole nerve recordings used for correction of footdrop in hemiplegic man," *IEEE Trans. Rehab. Eng.*, vol. 3, pp. 307–317, 1995.

[13] J. A. Hoffer, Y. Chen, K. D. Strange, and P. R. Christensen, "Nerve cuff having one or more isolated chambers," U. S. Patent 5,824,027, awarded Oct. 20, 1998.

[14] J. A. Hoffer, G. E. Loeb, and C. A. Pratt, "Single unit conduction velocities from averaged nerve cuff electrode records in freely moving cats," *J. Neurosci. Methods*, vol. 4, pp. 211–225, 1981.

[15] J. A. Hoffer, R. B. Stein, M. K. Haugland, T. Sinkjaer, W. K. Durfee, A. B. Schwartz, G. E. Loeb, and C. Kantor, "Neural signals for command control and feedback in functional neuromuscular stimulation: A review," *J. Rehab. Res. Dev.*, vol. 33, pp. 145–157, 1996.

[16] J. A. Hoffer, K. D. Strange, P. R. Christensen, Y. Chen, and K. Yoshida, "Multi-channel recordings from peripheral nerves: 1. Properties of multi-contact cuff (MCC) and longitudinal intra-fascicular electrode (LIFE) arrays implanted in cat forelimb nerves," in *Proc. IFESS/NP*, 1997, pp. 239–240.

[17] K. Hsu and D. M. Durand, "Determination of excitation thresholds of nerve fibers during magnetic stimulation," in *Proc. 18th IEEE/EMBS Annu. Int. Conf.*, 1996.

[18] B. K. Lichtenberg and C. J. De Luca, "Distinguishability of functionally distinct evoked neuroelectric signals on the surface of a nerve," *IEEE Trans. Biomed. Eng.*, vol. 26, pp. 228–237, 1979.

[19] W. B. Marks and G. E. Loeb, "Action currents, internodal potentials, and extracellular records of myelinated mammalian nerve fibers derived from node potentials," *Biophys. J.*, vol. 16, pp. 655–668, 1976.

[20] J. H. Meier, W. L. C. Rutten, and H. B. K. Boom, "Extracellular potentials from active myelinated fibers inside insulated and noninsulated peripheral nerve," *IEEE Trans. Biomed. Eng.*, vol. 45, pp. 1146–1153, 1998.

[21] M. Sahin and D. M. Durand, “Selective recording with a multi-contact nerve cuff electrode,” in *Proc. 18th IEEE/EMBS Annu. Int. Conf.*, 1996.
[22] M. Sahin, D. M. Durand, and M. A. Haxhiu, “Improved nerve cuff electrode recordings by sub-threshold anodic currents,” in *Proc. 17th IEEE/EMBS Annu. Int. Conf.*, 1995.
[23] T. Sinkjaer and J.-P. Micallef, “Sensors,” in *Restoration of Walking for Paraplegics: Recent Advancements and Trends*, A. Pedotti and M. Ferrarin, Eds. Milan, Italy: Edizioni Pro Juventute, 1992, pp. 251–254.
[24] R. B. Stein, D. Charles, L. Davis, J. Jhamandas, A. Mannard, and T. R. Nichols, “Principles underlying new methods for chronic neural recording,” *Can. J. Neurologic. Sci.*, pp. 234–244, 1975.
[25] R. B. Stein, T. R. Nichols, J. Jhamandas, L. Davis, and D. Charles, “Stable long-term recordings from cat peripheral nerves,” *Brain Res.*, vol. 128, pp. 21–38, 1977.
[26] R. B. Stein and K. G. Pearson, “Predicted amplitude and form of action potentials recorded from unmyelinated nerve fibers,” *J. Theor. Biol.*, vol. 32, pp. 539–558, 1971.
[27] R. B. Stein, P. H. Peckham, and D. B. Popovic, Eds., *Neural Prostheses: Replacing Motor Function After Disease or Disability*. New York: Oxford University Press, 1992.
[28] J. J. Struijk, “The extracellular potential of a myelinated nerve fiber in an unbounded medium and in nerve cuff models,” *Biophys. J.*, vol. 72, pp. 2457–2469, 1997.
[29] J. J. Struijk, M. K. Haugland, and M. Thomsen, “Fascicle selective recording with a nerve cuff electrode,” in *Proc. 18th IEEE/EMBS Annu. Int. Conf.*, 1996.
[30] J. J. Struijk, M. Thomsen, J. O. Larsen, and T. Sinkjaer, “Cuff electrodes for long-term recording of natural sensory information,” *IEEE Eng. Med. Biol.*, vol. 18, pp. 91–98, 1999.
[31] S. Sunderland, “The intraneural topography of the radial, median and ulnar nerves,” *Brain*, vol. 68, pp. 243–299, 1945.
[32] S. Sunderland and L. J. Ray, “The intraneural topography of the sciatic nerve and its popliteal divisions in man,” *Brain*, vol. 71, pp. 242–273, 1948.
[33] J. D. Sweeney, J. T. Mortimer, and D. M. Durand, “Modeling of mammalian myelinated nerve for functional neuromuscular stimulation,” in *Proc. 9th IEEE/EMBS Annu. Int. Conf.*, 1987.
[34] I. Tasaki, “A new measurement of action currents developed by single nodes of Ranvier,” *J. Neurophysiol.*, vol. 27, pp. 1199–1205, 1964.
[35] D. J. Tyler and D. M. Durand, “Chronic effect of a flat interface nerve electrode,” in *Proc. NIH Neural Prostheses Workshop,*, 1999.

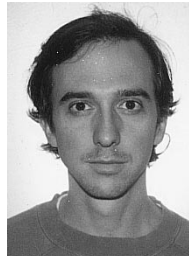

Javier Perez-Orive was born in Mexico City, Mexico, in 1970. He received the biomedical engineering degree from Universidad Iberoamericana, Mexico City, Mexico, in 1995. In 1998, he received the M.S. degree in biomedical engineering from Case Western Reserve University, Cleveland, OH. He is currently working towards the Ph.D.degree in the Computation and Neural Systems program at the California Institute of Technology, Pasadena, CA, where he is investigating the neural coding and decoding of information.

He has worked as an Associate Researcher in Biomedical Engineering in Instituto Nacional de Ortopedia/Centro Nacional de Rehabilitacion, Mexico City. His research interests include neural prostheses, computational neuroscience, and the study of neuronal coding and decoding of sensory information, both at the single cell and systems levels.

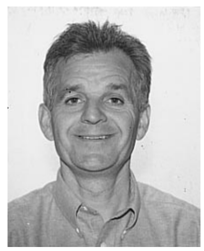

Dominique M. Durand (M’91) was born in Monbazillac, France, in 1951. He received the engineering degree from Ecole Nationale Superieure d’Electronique, Hydrolique, Informatique et Automatique de Toulouse, France, in 1973. In 1974, he received the M.S. degree in biomedical engineering from Case Reserve University, Cleveland, OH, and in 1982, received the Ph.D. degree in electrical engineering from the University of Toronto, Toronto, ON, Canada, from the Institute of Biomedical Engineering.

He worked several years at the Addiction Research Foundation of Toronto. Currently, he is Professor in the Departments of Biomedical Engineering and Neurosciences at Case Western Reserve University. His research interests are in neural engineering and include computational neuroscience, neurophysiology and control of epilepsy, nonlinear dynamics of neural systems, neural prostheses, and applied magnetic and electrical field interactions with neural tissue.

Dr. Durand received a NSF Young Investigator Presidential Award as well as undergraduate and graduate teaching awards. He is a Fellow of the American Institute for Medical and Biomedical Engineering.